MULTI-POINT CLUSTER OBSERVATIONS OF VLF RISERS, FALLERS AND HOOKS AT AND NEAR THE PLASMAPAUSE

J. S. Pickett[1], O. Santolík[2,1], S. W. Kahler[1], A. Masson[3], M. L. Adrian[4], D. A. Gurnett[1], T. F. Bell[5], H. Laakso[3], M. Parrot[6], P. Décréau[7], A. Fazakerley[8], N. Cornilleau-Wehrlin[9], A. Balogh[10], and M. André[11]

[1]Department of Physics and Astronomy, The University of Iowa, Iowa City, IA, USA; [2]Faculty of Mathematics and Physics, Charles University, Prague, Czech Republic; [3]RSSD of ESA, ESTEC, Noordwijk, The Netherlands; [4]Marshall Space Flight Center, Huntsville, AL, USA; [5]Starlab, Stanford University, Stanford, CA, USA; [6]LPCE/CNRS, Orleans, France; [7]LPCE et Université d'Orléans, Orléans, France; [8]Mullard Space Science Laboratory, University College, London, UK; [9]CETP/UVSQ, Velizy, France; [10]The Blackett Laboratory, Imperial College, London, UK; [11]Swedish Institute of Space Physics, Uppsala Division, Uppsala, Sweden

Abstract: The four Cluster Wideband (WBD) plasma wave receivers occasionally observe electromagnetic triggered wave emissions at and near the plasmapause. We present the remarkable cases of such observations. These triggered emissions consist of very fine structured VLF risers, fallers and hooks in the frequency range of 1.5 to 3.5 kHz with frequency drifts for the risers on the order of 1 kHz/s. They appear to be triggered out of the background whistler mode waves (hiss) that are usually observed in this region, as well as from narrowband, constant frequency emissions. Occasionally, identical, but weaker, emissions are seen to follow the initial triggered emissions. When all the Cluster spacecraft are relatively close (< 800 km, with interspacecraft separations of around 100–200 km), the triggered emissions are correlated across all the spacecraft. The triggered emissions reported here are observed near the perigee of the Cluster spacecraft (around 4–5 R_E) within about 20 degrees, north or south, of the magnetic equator at varying magnetic local times and generally at times of low to moderate Kp. In at least one case they have been observed to be propagating toward the magnetic equator at group velocities on the order of $5–9 \times 10^7$ m/s. The triggered emissions are observed in the region of steep density gradient either leading up to or away from the plasmasphere where small-scale density cavities are often encountered. Through analysis of images from the EUV instrument onboard the IMAGE spacecraft, we provide evidence that Cluster may sometimes be immersed in a low density channel or other complex

J. –A. Sauvaud and Z. Němeček (eds.),
Multiscale Processes in the Earth's Magnetosphere:From Interball to Cluster, 307-328.

structure at the plasmapause when it observes the triggered emissions. Examples of the various types of triggered emissions are provided which show the correlations across spacecraft. Supporting density data are included in order to determine the location of the plasmapause. A nonlinear gyroresonance wave-particle interaction mechanism is discussed as one possible generation mechanism.

Key words: triggered emissions; plasmapause; risers; fallers; hooks; Cluster observations.

1. INTRODUCTION

Triggered and discrete narrowband emissions have been observed on the ground and in space for decades (Smith and Nunn, 1998). These emissions are generally observed both inside and outside the plasmapause at L values ranging from about 2.5 to 10. They are observed primarily in the form of risers, fallers and upward and downward hooks, or combinations thereof [cf., Helliwell, (1965); Smith and Nunn, (1998)]. Discrete emissions have been defined as emissions having no obvious trigger source, whereas triggered emissions have a clearly recognizable trigger signal (Nunn et al., 1997). A review of the observations and generation theories of triggered emissions was contained in Matsumoto (1979) and Omura et al. (1991) who characterized these emissions as 1) being narrow bandwidth, usually less than 100 Hz; 2) having long durations, sometimes on the order of 1 s; 3) having large amplitudes which saturate at a level as much as 30 dB above that of the triggering signal; 4) having continuously sweeping frequency, typically at a rate of order kHz/s; and 5) taking place almost always within the plasmasphere. Triggered emissions are observed to be produced by constant-frequency wave (CW) transmissions from terrestrial VLF transmitters (Helliwell, 1965; Bell, 1985), by lightning VLF whistlers (Nunn and Smith, 1996), by magnetospheric lines and strong Power-Line Harmonic Radiation (PLHR) induction lines (Helliwell et al., 1975; Luette et al., 1979; Parrot and Zaslavski, 1996; Nunn et al., 1997) and by hiss (Smith and Nunn, 1998).

Discrete emissions have similar characteristics as triggered emissions but appear as isolated events, perhaps arising spontaneously because of high instability conditions in the plasma triggered by random noise, very weak PLHR, or unducted VLF signals (Nunn et al., 1997). They can be either ducted or unducted. VLF chorus is composed of a sequence of closely spaced, discrete emissions, often overlapping in time and most often consisting of rising tones (Helliwell, 1965). Thus chorus shares many of the characteristics of the more isolated discrete emissions. Often a background

of hiss is present when chorus is observed. For a review of chorus observations and theory, see Sazhin and Hayakawa (1992).

Several more recent studies have been published that deal with triggered, discrete and chorus emissions. These include, but are not limited to, LeDocq, et al. (1998), Trakhtengerts (1999), Bell et al. (2000), Trakhtengerts and Rycroft (2000), Meredith et al. (2001), Pasmanik, et al. (2002), Lauben et al. (2002), Santolík and Gurnett (2003), and Parrot et al. (2003). Several studies are ongoing at the present time to provide further understanding of the propagation characteristics of these emissions, as well as their generation mechanisms. For example, one surprising aspect of chorus was the discovery by Gurnett et al. (2001) that correlated chorus elements appear at different frequencies on the various Cluster spacecraft separated by distances of a few hundred km or less.

The main aim of this paper is to bring a multi-spacecraft perspective to the observations of triggered emissions in the form of risers, fallers, hooks and combinations thereof that are made on Cluster at and inside the plasmapause. We refer to these emissions as triggered emissions as they appear in many cases to be triggered from observable wave sources. In a few of the cases where the triggering emission is somewhat in doubt, the emissions might better be referred to as discrete since the individual risers, fallers and hooks are well isolated from one another. We begin by describing the suite of instruments on the Cluster and IMAGE spacecraft whose observations are the focus of this study. We show examples of the types of triggered emissions that are observed and their correlation across several spacecraft separated by hundreds of km. This is followed by a discussion of the observations in terms of their significance and of a possible generation mechanism.

2. INSTRUMENTATION

The primary observations discussed below are from the Cluster Wideband (WBD) plasma wave receiver (Gurnett et al., 1997) which makes a one-axis measurement of the electric or magnetic field using one 88 m dipole antenna or one of three orthogonal magnetic searchcoils. The electric antennas of the four Cluster spacecraft are always oriented close to the ecliptic plane and are spinning with a period of approximately 4 seconds. WBD continuously samples waveforms using a 9.5 kHz bandwidth filter with filter roll-off occurring at about 50 Hz on the low end and 9.5 kHz on the high end. It contains an automatic gain system, implemented in hardware, with gain update rate of 0.1 s, which helps to keep the high intensity triggered emissions within the dynamic range of the instrument

without clipping. The data are sampled at high time resolution, 36.5 μs, by transmitting the data directly to the Deep Space Network (DSN) ground stations located in Canberra, Australia and Goldstone, California, USA. WBD data on each spacecraft are obtained over approximately 4% of any one 57-hour Cluster orbit. All of the WBD data shown in this paper were obtained while the spacecraft were near perigee (4.0-4.5 Re). Typically, in this region of space WBD cycles between an electric antenna and a magnetic searchcoil antenna with a 42s/10s duty cycle, respectively. Since the onboard time counter only allows for absolute time accuracy to about 2 ms, WBD makes use of the ground receive time tags provided by DSN, which are accurate to 10 μs, in order to determine time delays between spacecraft.

In situ density measurements are obtained by the Whisper sounder (Décréau et al., 1997) provided the plasma frequency associated with that density falls within the frequency range of the instrument (80 kHz). The Whisper sounder is designed to provide an absolute measurement of the total plasma density by the means of a resonance sounding technique in the range of 0.2 – 80 cm^{-3}. These measurements are usually made for a period of about 3 s every 52 s during WBD operation. The EFW instrument measures electric fields and waves with two pairs of probes on wire booms in the spin plane of each satellite (the same probes used by WBD to make its wave electric field measurements). Each pair has a probe-to-probe separation of 88 m (Gustafsson et al., 1997). The potential of the probes with respect to the spacecraft is sampled at 5 samples/s, and this measurement can be used to estimate the plasma density. This technique can be used in all but the most tenuous magnetospheric plasmas traversed by Cluster where the spacecraft current balance becomes more sensitive to the energy of the ambient electrons (Pedersen et al., 2001, André et al, 2001). The lower time resolution density measurements from the Whisper Sounder have been used here to better calibrate the density values obtained from the higher time resolution EFW potential measurements. Simultaneous measurements of the waves using the two spin plane electric field antennas and the three magnetic searchcoils at frequencies between 8 Hz and 4 kHz are made by the STAFF-SA instrument (Cornilleau-Wherlin, 1997). STAFF-SA provides the complete auto- and cross-spectra over a frequency range of nine octaves, which are then analyzed to obtain the wave vector, Poynting vector, ellipticity and planarity of polarization. The averaged magnetic field measurements with a time resolution of 4 seconds that are used to calculate the electron cyclotron frequency and to determine each of the spacecraft's locations in a magnetic field aligned coordinate system are provided by the FGM instrument (Balogh et al., 1997). FGM consists of two triaxial fluxgate magnetometers, with one of the sensors located at the end of one of the two 5.2 m radial booms of the spacecraft and the other at 1.5 m inboard from the

end of the boom. Remote sensing of the plasmasphere is provided by the Extreme Ultraviolet Imager (EUV) located on the IMAGE spacecraft (Sandel et al., 2000). EUV is designed to image the distribution of plasmaspheric He^+ ions (typically plasmaspheric $He^+/H^+ \sim 0.1–0.2$) via resonant scattering of solar 30.4-nm UV radiation. Tuned specifically to detect the 30.4-nm resonance line of plasmaspheric He^+, EUV consists of three wide–field (30°) cameras such that the field-of-view (FOV) of the three cameras overlap slightly to form a fan-shaped instantaneous FOV of dimensions 84° x 30° (Sandel et al., 2000; 2001). As the IMAGE satellite proceeds through a single spin, the fan–shaped FOV of EUV sweeps across an 84° x 360° swath of sky recording the intensity of detected 30.4-nm radiation in an array of approximately 0.6° × 0.6° pixels. Since the plasmaspheric He^+ scattered 30.4-nm emission is an optically thin medium, the measured intensity is directly proportional to the He^+ column density along the line of sight through the plasmasphere. Each frame of EUV imaged data is produced from a 10-minute accumulation that encompasses 5–spins of the IMAGE satellite.

3. OBSERVATIONS

We present WBD observations of triggered emissions in the form of VLF risers, fallers and hooks from three different dates, March 11, 2002, June 23, 2003 and August 31, 2003, when Cluster was located at or near the plasmapause. Table 1 shows the separation distances between the four Cluster spacecraft along the direction of the magnetic field and perpendicular to that direction. The Kp index for each of these three dates was moderate to low at 2-, 4, and +1, respectively. The Kp index is probably important as it is based on processes that have been shown to affect the location of the plasmapause (Moldwin et al., 2002).

Table 1. Spacecraft separations along and across B for time periods shown in Figures 1, 4 and 8.

	SC1-SC2 (km)	SC1-SC3 (km)	SC1-SC4 (km)	SC2-SC3 (km)	SC2-SC4 (km)	SC3-SC4 (km)
Mar. 11, 2002						
// to B	105	162	216	57	111	54
ζ to B	151	195	306	71	166	111
Jun. 23, 2003						
// to B					23	
ζ to B					121	
Aug. 31, 2003						
// to B	464	560	825	96	361	265
ζ to B	518	421	747	98	243	333

3.1 March 11, 2002

We begin our survey of the triggered emissions by showing an example from March 11, 2002 when the four spacecraft were relatively close to each other (~100 km separations). Figure 1 is a typical frequency, in kHz, vs. time, in UT hours:minutes:seconds, spectrogram with gray scale indicating electric field power spectral density. The panels from top to bottom show the WBD data from Cluster spacecraft (SC) 1 through 4, respectively. This particular example spans a time period of 4 seconds in which triggered emissions in the form of linked risers and fallers, or upward and downward

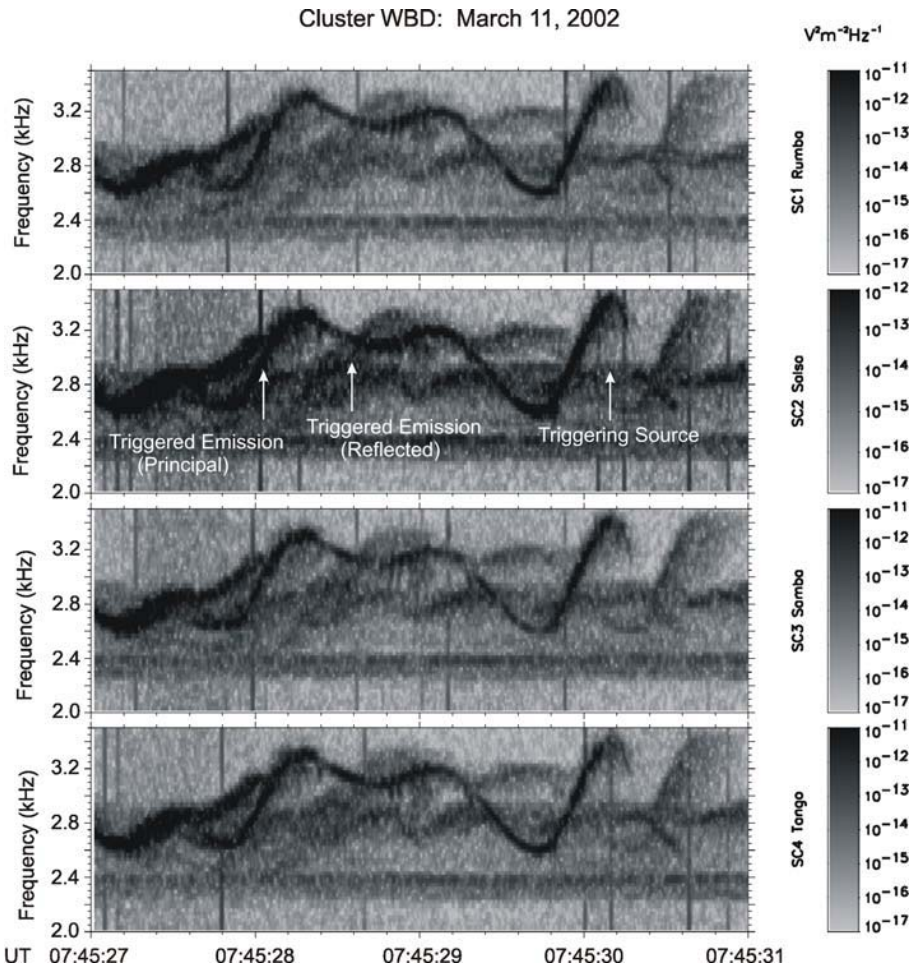

Figure 1. Cluster WBD spectrogram of linked risers and fallers (or upward and linked downward hooks) observed on all four Cluster spacecraft on March 11, 2002. The hooks appear to be triggered out of a constant frequency wave of frequency about 2.8 kHz.

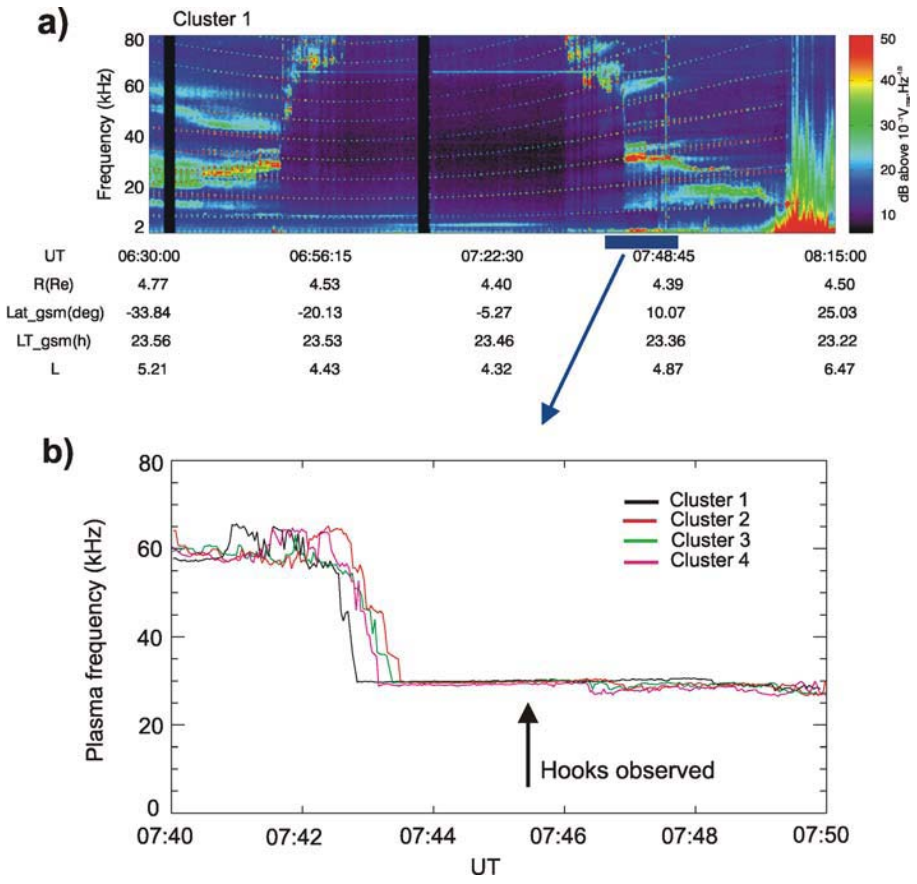

Figure 2. Profile of the electron plasma frequency constructed using the Whisper sounder measurements onboard Cluster 1 on March 11, 2002. a) The power spectrogram showing both the active and the passive spectra. b) Detail of the profile of the electron plasma frequency close to the time interval where the WBD instrument measures triggered emissions (indicated by an arrow).

hooks, are observed to form a nearly sinusoidal signature in the frequency domain. The triggered emissions span the frequency range of about 2.5-3.5 kHz and appear to be triggered out of a narrowband, nearly constant frequency emission observed at about 2.8 kHz. The triggered emissions are well-correlated across all four spacecraft. One particularly interesting feature of these triggered emissions is their reappearance, suggestive of reflection of the principal emission, approximately ½ s after the initial principal intense emissions, but at a much reduced amplitude and slightly more diffuse. These data were obtained while the spacecraft were at 4.4 R_E, 19.3º magnetic latitude, 23.3 hours magnetic local time and 4.9 L-shell. Although not shown in Figure 1, WBD data obtained just prior to 07:45:00, while the instrument

was sampling with the magnetic searchcoil as a sensor for 10 s, clearly show that the triggered emissions have magnetic components where the E/B ratio is higher for the waves from which the emissions are triggered than for the triggered emissions themselves. In addition, the overall intensity of the triggered emissions is much higher than the waves from which they are triggered.

The in situ density profile for this March 11, 2002 triggered emission case can be obtained from measurements of the Whisper sounder. Figure 2a shows the power spectrogram from Cluster 1. Both active and passive regimes of the instrument are combined. The slowly varying dotted lines are interpreted as electron cyclotron harmonics appearing when the active sounding mode takes place (once per 52 seconds). Interpretation of these measurements in terms of the local plasma frequency is shown in Figure 2b. We show here a small subinterval of time between 07:40 and 07:50 UT, when the spacecraft exited from the plasmasphere. This time interval is indicated by a bar under the spectrogram in Figure 2a. In Figure 2b we combine results from all four Cluster spacecraft (distinguished per the code in the upper right-hand corner). The time when the triggered emissions were observed on the WBD instrument is shown by an arrow. These emissions were observed outside of the plasmasphere in the plateau region at a density around 10 cm^{-3}. Other observations of triggered emissions during this pass are again localized in the low-density region from 07:47 to 07:49 UT.

An observation of the plasmasphere recorded by the IMAGE EUV instrument post–Cluster measurements is presented in Figure 3. Figure 3(a) shows the EUV image taken at 11:55 UT on 11 March 2002 with the direction to the sun annotated with an arrow. The image indicates that the Cluster measurements presented in Figure 1 and 2 were made in the presence of a complex plasmapause/plasmasphere region characterized by a distinct plasmapause and an embedded low-density channel located radially inward of the plasmapause. The low-density channel is observed to extend from dusk, through Earth's shadow, and on toward dawn. The salient plasmaspheric features of the observation are annotated in Figure 3(b). These features are mapped onto the equatorial plane of the solar magnetic (SM) coordinate system in Figure 3(c) and presented in relation to the orbit of the Cluster tetrahedron from 04:00–10:00 UT projected onto this plane (note that from the perspective of IMAGE EUV at 11:55 UT, the ~100-km separation of the individual Cluster spacecraft is not discernable). The segment of the Cluster orbit spanning the measurements presented in Figures 1 and 2 (07:27–08:03 UT) is highlighted (from triangle to square). Had the Cluster/IMAGE observations been concurrent, Figure 3(c) would indicate that Cluster encountered the plasmasphere within the region of Earth's

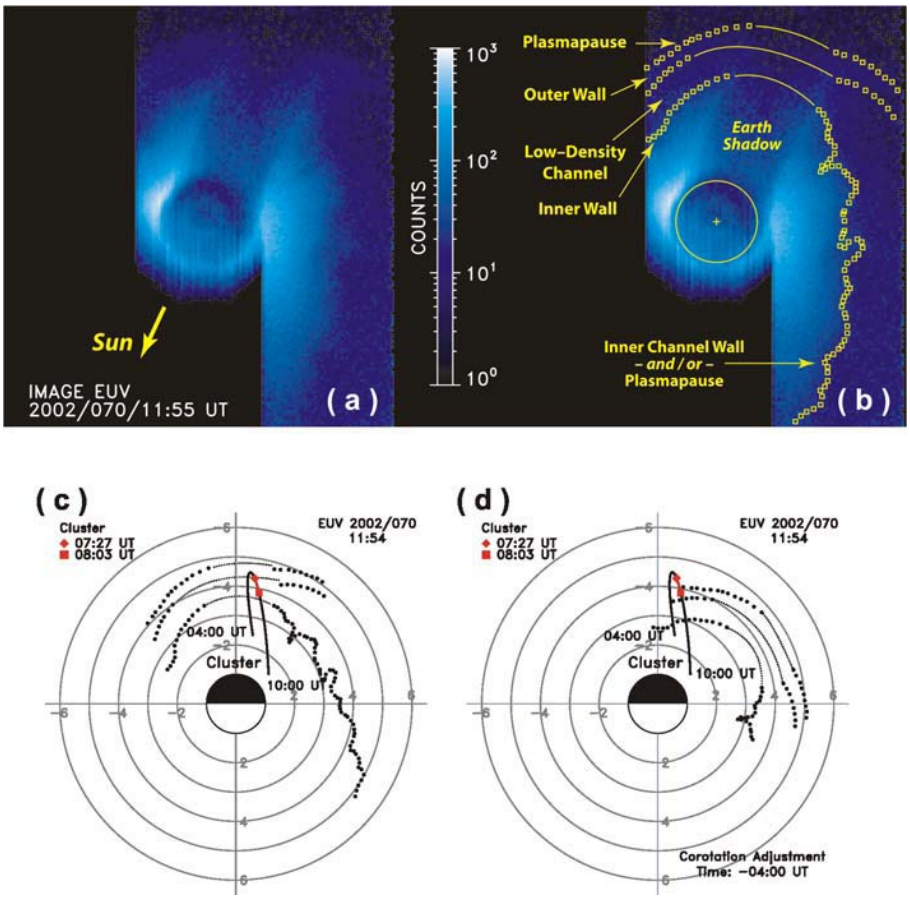

Figure 3. Data from the IMAGE EUV instrument. (a) EUV image taken at 11:55 UT on 11 March 2002 with the direction to the sun annotated with an arrow; (b) Annotation of (a) with the salient plasmaspheric features; (c) plasmaspheric features noted in (b) mapped onto the equatorial plane of the solar magnetic (SM) coordinate system and presented in relation to the projection of the Cluster orbit from 04:00–10:00 UT onto this plane; (d) remapping of observed plasmaspheric features under the assumption of 4-hours of corotation. Remapping results in Cluster immersed in the main trough and transiting the plasmapause and constrained by the plasmapause and outer wall of the low–density channel at the time of WBD–observed triggered emissions.

shadow and would suggest that the WBD–observed triggered risers/fallers had occurred as Cluster transited the outer wall of, and into, the low–density channel. However, the Cluster/IMAGE observations are not concurrent; the IMAGE EUV observation occurs ~4-hours post–Cluster. Assuming plasmapause stability, plasmaspheric feature constraint to dipole field lines, and corotation, the plasmaspheric features observed by EUV, and presented in Figure 3(c), can be remapped back in time to concurrence with the

presented Cluster observations. Figure 3(d) presents the remapping of observed plasmaspheric features under the assumption of 4-hours of corotation. Remapping back in time results in Cluster immersed in the main trough and transiting the plasmapause, being constrained by the plasmapause and outer wall of the low–density channel at the time of WBD–observed triggered emissions. The remapping is consistent with density data observed *in–situ* by Cluster (Figure 2). Together with the observed *in–situ* density data, the EUV image may help explain the appearance of the triggered emissions observed by WBD in proximity to the density gradient of the plasmapause.

3.2 June 23, 2003

Next we turn to an example of some well-isolated risers and hooks observed on June 23, 2003 when the Cluster spacecraft were in the middle of their major maneuver period of going from large spacecraft separations (order of 5,000 km) to their small separations (order of 200 km). At this time the two pairs of spacecraft (1,3 and 2,4) were separated by about 35,000 km, while the distances between spacecraft 2 and 4 were less than 150 km. Because of the large distance between the two pairs, we resort to showing only the data from one pair (2 and 4) in order to observe the correlation of the triggered emissions. Figure 4 is a spectrogram in the same format at Figure 1 showing the WBD data from these two spacecraft while they were at 4.4 R_E, 12.1º magnetic latitude, 16.8 hours magnetic local time and 4.6 L-shell. Clearly, the isolated riser/hook combinations are correlated between the two spacecraft in the frequency domain, although the riser/hook combinations are considerably more intense on SC2. This suggests that the source may be closer to SC2. The frequency range of these emissions is about 2 to 3.5 kHz and their frequency drift is on the order of 1 kHz/s. In this case the riser/hook combinations appear to be triggered out of the low frequency waves (hiss) that cover the frequency range from the lowest frequency measured (about 50 Hz) up to about 2 kHz. Note also the presence of secondary triggered emissions from the risers, some of which are seen only on one spacecraft, such as the one centered at 03:45:13 UT on SC4.

In order to determine the direction of propagation of these isolated riser/hook combinations, it is necessary to go to the time domain to do the analysis since the spectrograms are created using FFTs which average over time scales much larger than the delay times. We have chosen the riser/hook centered on 03:45:13 UT for our analysis. Figure 5 shows the filtered waveforms for 0.5 seconds beginning at 03:45:13 UT. Plotted on the vertical axis are the calibrated electric field amplitudes, in mV/m, of the waveforms

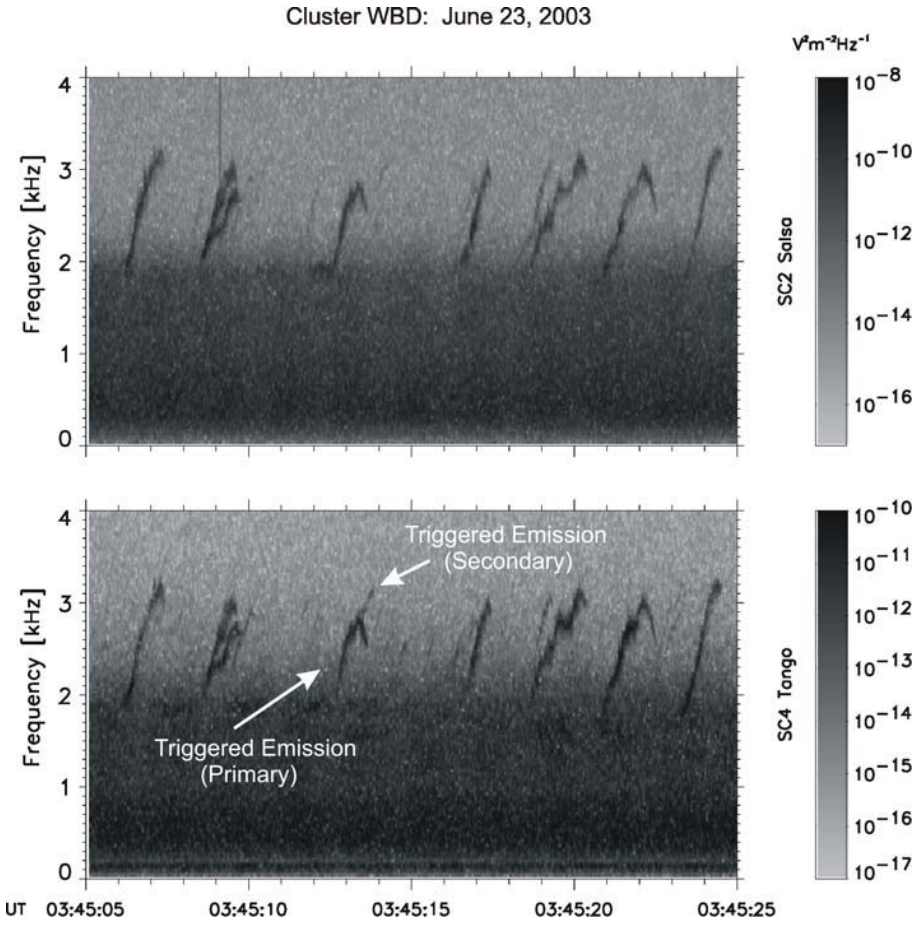

Figure 4. Cluster WBD spectrogram of riser/hook combinations observed on June 23, 2003 on two Cluster spacecraft. The riser/hook combinations appear to be triggered out of the hiss that cuts off around 2 kHz.

Table 2. Delay times associated with event times shown in Figure 5.

	Correlation Event Time		
Event Number	SC2 (UT)	SC4 (UT)	Delay Time (s)
1	03:45:13.10839	03:45:13.11284	0.00445
2	03:45:13.21639	03:45:13.21990	0.00351
3	03:45:13.36511	03:45:13.36839	0.00328
4	03:45:13.40467	03:45:13.40767	0.00300

vs. time, in s, obtained by WBD on SC2 (top panel) and SC4 (bottom panel). This figure makes it clear that SC2 observes higher amplitude waves than SC4 as stated above. We have chosen to use a Finite Impulse Response (FIR) filter over the 2-3 kHz frequency range in order to remain outside the frequency range of the intense low frequency waves and yet fully contain a major portion of the riser portion of the triggered emission. We have pointed out four different correlated wave packet intervals for further analysis by putting a grey-shaded box around them and numbering them 1 through 4 in each of the two panels. For each of the four chosen wave packets we have calculated a delay time of arrival at SC4 from SC2 using the peaks as our reference. The results of these calculations are shown in Table 2. Notice that the delay time, which varies from about 3 to 4.5 ms, decreases with time. Events 1 and 2 are from a time when the riser frequency is increasing.

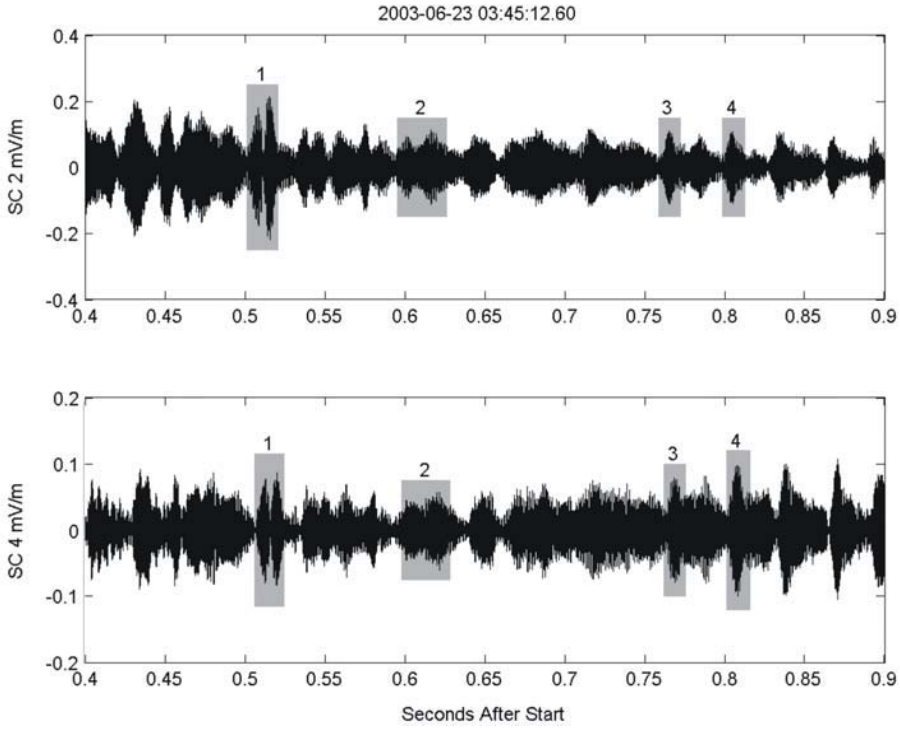

Figure 5. FIR-filtered waveform in the frequency band of 2–3 kHz of the riser/hook combination observed around 03:45:13 on June 23, 2003. Note the good correlations of the waveforms across the two spacecraft, which are used to obtain a time delay (see Table 2). In this case the riser/hook combination is seen first on SC2.

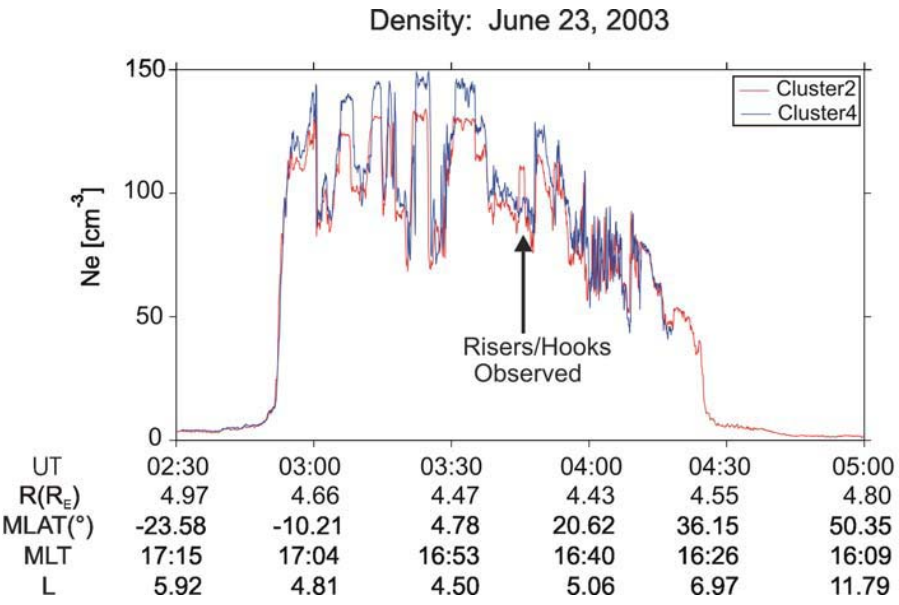

UT	02:30	03:00	03:30	04:00	04:30	05:00
$R(R_E)$	4.97	4.66	4.47	4.43	4.55	4.80
MLAT(°)	-23.58	-10.21	4.78	20.62	36.15	50.35
MLT	17:15	17:04	16:53	16:40	16:26	16:09
L	5.92	4.81	4.50	5.06	6.97	11.79

Figure 6. Electron density profile constructed using primarily EFW spacecraft potential measurements on June 23, 2003. The arrow indicates the time of the WBD measurements of triggered emissions, this being inside a broader localized density cavity in or near the plasmapause.

Events 3 and 4 are from a time after the peak of the hook when frequency is starting to decrease slightly. Although the spacecraft are getting closer to each other at this time, the closing distance is not sufficient to account for the decreasing delay times. The error in the time measurement is also not sufficient to account for the decreasing delay times. At this time SC2 is farther from the earth than SC4. SC2 is also at higher magnetic latitude than SC4. Since SC2 observes the wave packets first, the group velocity of this riser-hook combination must have a positive projection in the direction of the SC2-SC4 separation vector, i.e., in the direction toward the Earth and toward the magnetic equator. The same is true for the other risers/hooks observed in Figure 4. Based on the separation distance along the direction of the magnetic field as shown in Table 1 and the delay times shown in Table 2, and an assumption that these electromagnetic triggered emission waves are traveling along, or nearly along, the local magnetic field, we find that their group velocity is on the order of 6-9 x 10^7 m/s directed toward the magnetic equator. Cold plasma theory predicts for a wave of this frequency a group speed of 2 x 10^7 m/s (Stix, 1992).

The density profile for this encounter is shown in Figure 6 and is annotated using the ephemeris of Cluster 2. Because the density during most of this time period is above the range of Whisper (80 cm-3), EFW spacecraft

potential measurements have primarily been used to obtain a density, plotted in cm^{-3} along the vertical axis, vs. time, in hours:minutes along the horizontal axis. The two traces are coded by spacecraft as shown in the upper right-hand corner. The density values clearly indicate that the Cluster spacecraft encountered a commonly observed localized region of highly–structured dense plasma in the local time sector ~1600–1700 MLT between 4–7 R_E (Moldwin et al., 1994). The time of the riser/hook combination observations by WBD is indicated by an arrow, and is consistent with the spacecraft being located within one of the several broader localized density cavities within this localized region of dense plasma, even though SC2 is embedded in a narrower localized density enhancement.

The STAFF-SA data that cover the time period of the risers observed by WBD are shown in Figure 7. We show the data of SC2 where the emissions are more intense. The data of SC4 are not shown but lead to similar results. The upper two panels demonstrate that both the hiss below 2 kHz and triggered emissions between 2 and 3 kHz are electromagnetic waves. We have verified that the enhancements of the intensity of hiss between 03:45 and 03:46, and after 03:48 are directly correlated with the density enhancements seen for Cluster 2 in Figure 6. This most probably corresponds to ducting of these waves by the density enhancements. Additional analysis shows that the waves are right-hand polarized consistent with their propagation in the whistler mode (not shown). Panel (c) represents results of analysis of the wave vector direction using singular value decomposition (SVD) of the magnetic cross-spectral matrix (Santolík et al., 2003). The wave vector of the hiss and triggered emissions is found to be within 20-30 degrees of the direction of the stationary magnetic field. Panel (d) shows the electromagnetic planarity estimator (Santolík et al., 2003) indicating if the waves propagate close to one single direction (values close to 1) or if the energy is distributed between antiparallel wave normals (values close to 0). The results at frequencies above 1 kHz where the electromagnetic planarity estimator gives values of 0.7 indicate that wave vectors are rather concentrated around one single direction. Finally, panel (e) shows the component of the Poynting flux parallel to the stationary magnetic field normalized by its standard deviation (Santolík et al, 2001). Positive values obtained for the hiss and triggered emissions signify that these waves propagate approximately in the direction of the stationary magnetic field, i.e., from the magnetic equator toward higher magnetic latitudes. For some cases of short-duration triggered emissions at higher frequencies, however, we cannot exclude opposite propagation since the results are not statistically reliable.

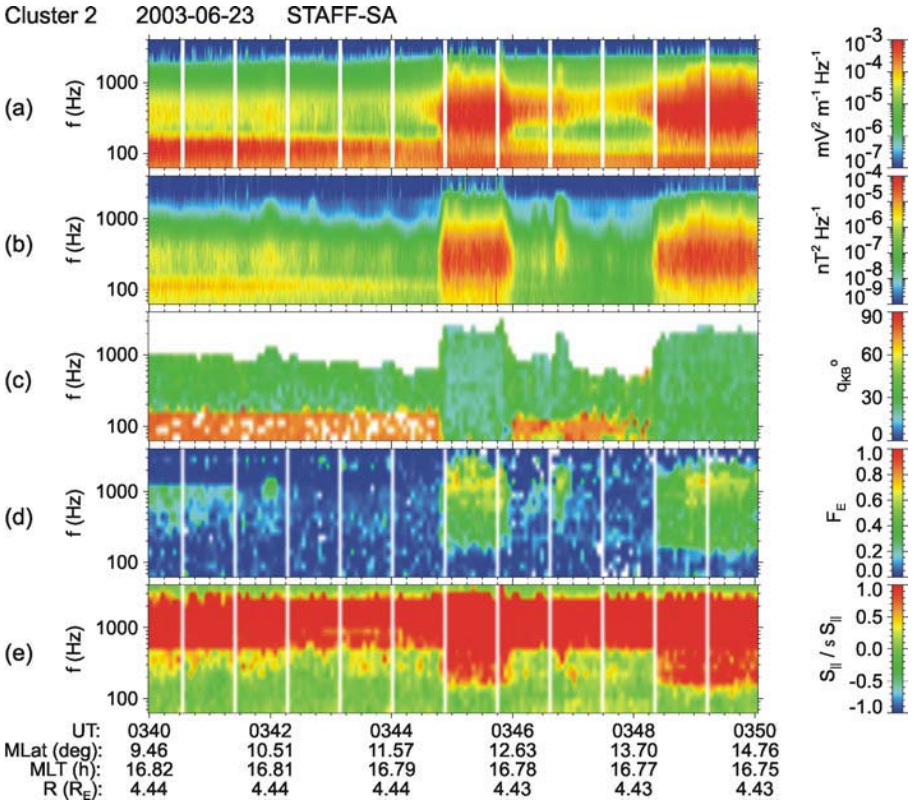

Figure 7. Time-frequency spectrograms measured by the STAFF-SA instrument onboard SC2 on June 23, 2003. (a) Sum of the power spectral densities of the two orthogonal electric components in the spin plane of the spacecraft. (b) Sum of the power spectral densities of the three orthogonal magnetic components. (c) Angle between the wave vector and the stationary magnetic field obtained from the cross-spectral analysis of the magnetic components using the SVD method. (d) Estimate of the electromagnetic planarity of wave fluctuations obtained using the SVD analysis. (e) Parallel component of the Poynting flux normalized by its standard deviation. Position of the spacecraft is given on the bottom, MLat being the magnetic dipole latitude in degrees, MLT being the magnetic local time in hours, and R being the radial distance in Earth radii.

3.3 August 31, 2003

As a final example, we show in Figure 8 a series of correlated risers, centered at 2 kHz, that were observed on August 31, 2003 at around 02:25 UT and that range in frequency from about 1.5 kHz up to about 2.5 kHz with frequency drifts on the order of 1 kHz/s. They appear to arise out of a lower frequency hiss-type emission whose upper cutoff frequency is about 1.8 kHz

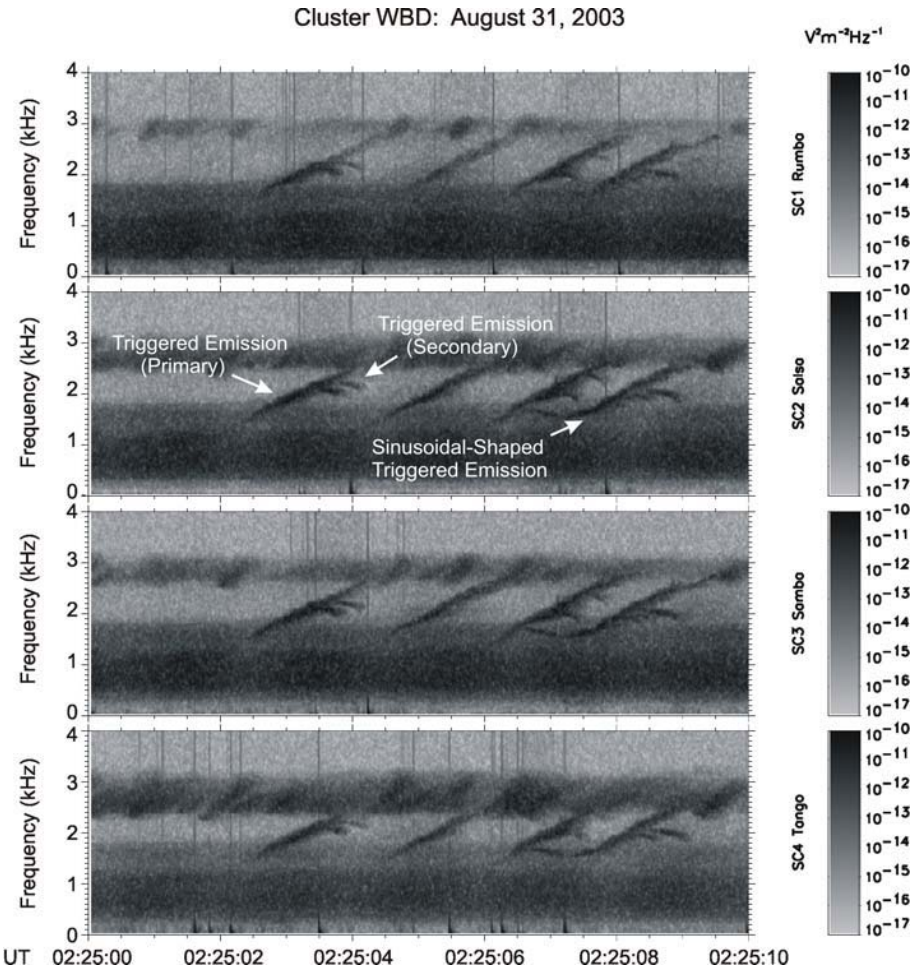

Figure 8. Cluster WBD spectrogram of risers observed on August 31, 2003 on all four Cluster spacecraft. The risers appear to be triggered out of the hiss.

and extend up into a band of more structured emission centered at about 2.9 kHz. Note also the secondary triggers coming off some of the risers, e.g., at 02:25:04 UT and the presence of a sinusoidal-shaped trigger starting around 02:25:07 UT, similar to those observed on March 11, 2002. The risers observed on August 31, 2003 appear to be triggered out of the diffuse plasma waves observed over the frequency range of 200 Hz to 1.8 kHz and be weakest on SC1 (perhaps furthest from source).

Table 1 shows that the maximum separation distance of the different spacecraft was more than 800 km both in the direction along the DC magnetic field and perpendicular to it. The maximum absolute separation is over 1100 km in this case. It is important to note that the triggered emissions

are still well correlated in Figure 8, even for those relatively large maximum separations between the points of observation.

On this date the four spacecraft were located at approximately 4.6 R_E, -19.3º magnetic latitude, 12.5 hours magnetic local time and L-shell of 5.2. The density profile shown in Figure 9 (same format as Figure 6, but using the ephemeris of Cluster 1) indicates that these triggered emissions were observed during entry into a post–noon localized, highly–structured region of dense plasma (Chappell et al., 1971) with the emissions occurring in the region of steepest density gradient (see arrow). Well defined density modulations appear during that time in the Whisper data at higher time resolution (not shown).

4. DISCUSSION

The Cluster WBD instrument has obtained multi-spacecraft measurements of the various types of triggered and discrete emissions that have long been observed on the ground and in space by one spacecraft. Upward and downward hooks, or linked risers and fallers, of the type shown in Figure 1 look very similar to those obtained at Halley station, Antarctica

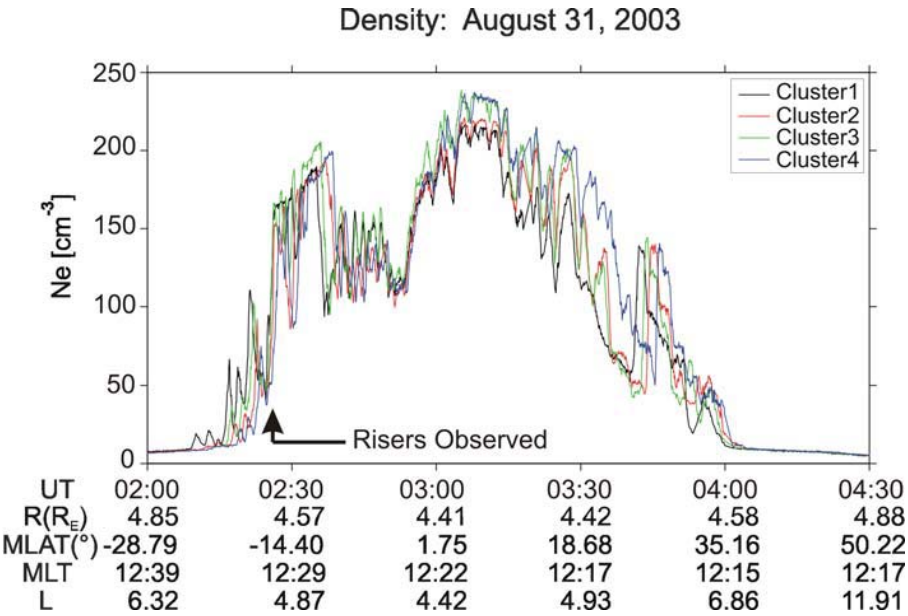

Figure 9. Electron density profile constructed using Cluster Whisper Sounder and EFW spacecraft potential measurements on August 31, 2003. The arrow indicates the time of the WBD measurements of the risers, this occurring on the steep density gradient on plasmasphere entry.

shown in Figure 1(e) of Smith and Nunn (1998). Likewise, the risers with downward hooks that arise out of the hiss as shown in Figure 4 look very similar to those which rise out of the hiss as shown in Figure 1(g) of Smith and Nunn (1998). Using the Cluster multispacecraft capability, we have found that the triggered and discrete emissions are often observed to be correlated across distances as great as 800 km across and along the magnetic field direction. Santolík and Gurnett (2003) found a significant correlation at distances of a few hundred km, but the correlation coefficient decreased with a characteristic scale of ~100 km across the magnetic field direction. They used WBD chorus data obtained under disturbed (high Kp) conditions in the low density region outside the plasmapause. Thus, it appears that correlation distances may be shorter well outside the plasmapause than inside based on these two studies. Statistical studies of these correlation lengths have now been started in order to determine what these correlation lengths are, both inside and outside the plasmapause, and the dependence, if any, on solar wind pressure and interplanetary magnetic field configuration.

Another characteristic of the triggered emissions discussed in this study is that they sometimes propagate toward Earth and the magnetic equator as observed on June 23, 2003. Chorus has generally been shown to propagate away from the equator (LeDocq et al., 1998), although Parrot et al. (2003) have shown that there is a reflected component of chorus that propagates back toward the equator after lower hybrid resonance reflection. Likewise, the reappearance on March 11, 2002 of the triggered emissions at much lower intensity approximately ½ s after the appearance of the principal triggered emissions observed by Cluster suggests that a series of linked upward and downward hooks may also be reflected. Supposing a constant group speed of 2 x 10^7 m/s obtained from the cold plasma theory, the delay of 0.5 s gives a rough estimate of the distance of ~1 Earth radius to a reflection point. Future research will attempt to identify the location of the reflection point using a ray tracing algorithm.

The difference in the group velocity obtained for the riser/hook combination on June 23, 2003 and that obtained from cold plasma theory is still under investigation. The error in the time delay measurements could not account for this difference. The possibility exists that there may be a warmer particle population embedded in this highly-structured, generally cold plasmaspheric plasma which could account for this difference in the measured velocity to the theoretical one. Analysis of future events with simultaneous particle measurements should help resolve this problem. In addition, the reason for the trend observed on the same date of decreasing time delays with time for the riser/hook combinations is also still under investigation. A Doppler shift could not account for this trend since the

average phase speeds of the triggered emissions is on the order of 1.5 x 10^7 m/s.

Several studies discussed the generation mechanism of the narrowband and/or the fine structures (e.g., Lutomirski and Sudan, 1966; Melrose, 1986; Nunn et al, 1999; Willes, 2002). Regarding a generation mechanism for the triggered emissions observed on Cluster, we have briefly explored the generation mechanism proposed by Bell et al. (2000) for triggered emissions observed on Polar inside the plasmasphere. This generation mechanism involves a nonlinear gyroresonance interaction between the energetic electrons and the VLF waves, which in the Cluster case would be VLF hiss and constant-frequency emissions. A cursory analysis of the Cluster PEACE (Johnstone et al., 1997) electron data suggests that there may be enough amplification of the waves as they propagate across the magnetic equator in the presence of 15-26 keV electrons to produce the triggered emissions. However, analysis of these data have literally just begun on Cluster for these types of studies since PEACE electron data have just started (in mid 2003) to be taken consistently through Cluster perigee. Thus, there is much work still ongoing in this area.

5. SUMMARY AND CONCLUDING REMARKS

A summary of our main findings with respect to triggered emissions observed on Cluster multi-spacecraft at or near the plasmapause using the Wideband plasma wave receiver as a detector is as follows:

- The VLF triggered emissions are observed on Cluster as electromagnetic fine-structured risers, fallers, hooks and combinations thereof in the Fourier-transformed spectrograms in the frequency range of 1.5-3.5 kHz with frequency drifts on the order of 1 kHz/s.
- Secondary triggered emissions are sometimes observed to be triggered by the primary triggered emissions.
- Occasionally the principal triggered emissions are observed less than 1 s later at greatly reduced amplitudes.
- The triggered emissions are observed within about 20 degrees north and south of the magnetic equator at around 4-5 R_E, all magnetic local times, and L-shells of 4-6.
- Correlation distances are as great as about 800 km both along and cross B.
- The triggered emissions are seen propagating both toward and away from the magnetic equator at group velocities less than 1 x 10^8 m/s.
- The triggers appear to be hiss and narrowband, constant-frequency type emissions.

Cluster's orbit has proven to be very advantageous for obtaining observations of triggered emissions in the form of VLF risers, fallers and hooks since its perigee around 4 R_E is nearly at the magnetic equator and often cuts through at the plasmapause, or just inside or outside of it, at L-shells around 4-6. Thus, this orbit combined with the multi-spacecraft capability promises to provide even more discoveries and a greater understanding of these intense emissions and their connection to solar activity and changes in interplanetary magnetic fields.

ACKNOWLEDGMENTS

This work was supported under NASA/Goddard Space Flight Center Grant No. NAG5-9974. We thank all of the many groups on the European side for their part in obtaining the WBD data (ESA, ESTEC, ESOC, JSOC, Sheffield University, and the Cluster Wave Experiment Consortium), as well as those on the U.S. side (JPL/DSN). We also thank ESA and NASA for valuable analysis support tools, namely, CSDSWeb, SSCWeb and CDAWeb. The authors also wish to thank B.R Sandel and the IMAGE/EUV team at the University of Arizona for their assistance in the processing and analysis of EUV data.

REFERENCES

André, M., Behlke, R., Wahlund, J.-E., Vaivads, A., and Eriksson, A.-I., 2001, Multi-spacecraft observations of broadband waves near the lower hybrid frequency at the Earthward edge of the magnetopause, *Ann. Geophys.* **19**:1471–1481.

Balogh, A., Dunlop, M. W., Cowley, S. W. H., Southwood, D. J., Thomlinson, J. G., et al, 1997, The Cluster Magnetic Field Investigation, *Space Sci. Rev.* **79**:65–92.

Bell, T. F., 1985, High amplitude VLF transmitter signals and associated sidebands observed near the magnetic equatorial plane on the ISEE 1 satellite, *J. Geophys. Res.* **90**:2792–2795.

Bell, T. F., Inan, U. S., Helliwell, R. A., and Scudder, J. D., 2000, Simultaneous triggered VLF emissions and energetic electron distributions observed on POLAR with PWI and HYDRA, *Geophys. Res. Lett.* **27**(A2):165–168.

Chappell, C.R., Harris, K. K., and Sharp, G. W., 1971, The dayside of the plasmasphere, *J. Geophys. Res.* **76**:7632–7647.

Cornilleau-Wehrlin, N., Chauveau, P., Louis, S., Meyer, A., and Nappa, J. M., 1997, The Cluster Spatio-Temporal Analysis of Field Fluctuations (Staff) experiment, *Space Sci. Rev.* **79**:107–136.

Décréau, P. M. E., Fergeau, P., Krasnosels'kikh, V., Lévêque, M., Martin, Ph., et al., 1997, WHISPER, a resonance sounder and wave analyser: performances and perspectives for the Cluster mission, *Space. Sci. Rev.* **79**:157–193.

Gurnett, D. A., Huff, R. L., and Kirchner, D. L, 1997, The Wide-band plasma wave investigation, *Space Sci. Rev*. **79**:195–208.

Gurnett, D. A., Huff, R. L., Picket, J. S., Person, A. M., Mutel, R. L., et al., 2001, First results from the Cluster Wideband plasma wave investigation, *Ann. Geophys.* **19**:1259–1272.

Gustafsson, G., Bostrom, R., Holback, B., Holmgren, G., Lundgren, A., et al., 1997, The electric field and wave experiment for the Cluster mission, *Space Sci. Rev.* **79**:137–156.

Helliwell, R. A., 1965, *Whistlers and Related Ionospheric Phenomena*, Stanford University Press, Stanford, California.

Helliwell, R. A., Katsufrakis, J. P., Bell, T. F., and Raghuram, R., 1975, VLF line radiation in the earth's magnetosphere and its association with power system radiation, *J. Geophys. Res.* **80**:4249–4258.

Johnstone, A. D., Alsop, C., Burge, S., Carter, P. J., Coates, A. J., et al., 1997, Peace: a Plasma Electron and Current Experiment, *Space Sci. Rev*. **79**:351–398.

Lauben, D. S., Inan, U. S., Bell, T. F., and Gurnett, D. A., 2002, Source characteristics of ELF/VLF chorus, *J. Geophys. Res*., **107**(A10):1429, doi: 10.1029/2000JA003019.

LeDocq, M. J., Gurnett, D. A., and Hospodarsky, G. B., 1998, Chorus source locations from VLF Poynting flux measurements with the Polar spacecraft, *Geophys. Res. Lett.* **25**:4063–4066.

Luette, J. P., Park, C. G., and Helliwell, R. A., 1979, The control of the magnetosphere by power line radiation, *J. Geophys. Res*. **84**:2657–2660.

Lutomirski, R. F, and Sudan, R. N., 1966, Exact Nonlinear Electromagnetic Whistler Modes, *Phys. Rev.* **147**:156–165.

Matsumoto, H., 1979, Nonlinear whistler-mode interaction and triggered emissions in the magnetosphere: a review, in: *Wave Instabilities in Space Plasmas*, P. J. Palmadesso and K. Papadopoulos, eds., D. Reidel, Dordrecht, pp. 163.

Melrose, D. B., 1986, A phase-bunching mechanism for fine structures in auroral kilometric radiation and Jovian decametric radiation, *J. Geophys. Res.* **91**:7970–7980.

Meredith, N. P., Horne, R. B., and Anderson, R. R., 2001, Substorm dependence of chorus amplitudes: implications for the acceleration of electrons to relativistic energies, *J. Geophys. Res.* **106**:13,165–13,178.

Moldwin, M.B., Thomsen, M. G., Bame, S. J., McComas, D. J., and Moore, K. R., 1994, An examination of the structure and dynamics of the outer plasmasphere using multiple geosynchronous satellites, *J. Geophys. Res*. **99**:11,475–11,481.

Moldwin, M. B., Downward, L., Rassoul, K., Amin, R. and Anderson, R. R., 2002, A new model of the location of the plasmapause: CRRES results, *J. Geophys. Res.* **107**(A11):1339, doi: 10.1029/2001JA009211.

Nunn, D. and Smith, A. J., 1996, Numerical simulation of whistler-triggered VLF emissions observed in Antarctica, *J. Geophys. Res.* **101**(A3):5261–5277.

Nunn, D., Omura, Y., Matsumoto, H., Nagano, I., and Yagitani, S., 1997, The numerical simulation of VLF chorus and discrete emissions observed on the Geotail satellite using a Vlasov code, *J. Geophys. Res.* **102**(A12):27,083–27,097.

Nunn, D., Manninen, J., Turunen, T., Trakhtengerts, V., and Erokhin, N., 1999, On the nonlinear triggering of VLF emissions by power line harmonic radiation, *Ann. Geophys*. **17**:79–94.

Omura, Y., Nunn, D., Matsumoto, H. and Rycroft, M. J., 1991, A review of observational, theoretical and numerical studies of VLF triggered emissions, *J. Atmos. and Terres. Phys.* **53**(5):351–368.

Parrot, M., and Zaslavski, Z., 1996, Physical mechanisms of man made influences on the magnetosphere, *Surveys in Geophysics* **17**:67–100.

Parrot, M., O. Santolik, N. Cornilleau-Wehrlin, M. Maksimovic, and C.C. Harvey, 2003, Magnetospherically reflected chorus waves revealed by ray tracing with CLUSTER data, *Ann. Geophys.* **21**:1111–1120.

Pasmanik, D. L., Demekhov, A. G., Nunn, D., Trakhtengerts, V. Y., and Rycroft, M. J., 2002, Cyclotron amplification of whistler-mode waves: A parametric study relevant to discrete VLF emissions in the Earth's magnetosphere, *J. Geophys. Res.* **107**(A8):1162, doi: 10.1029/2001JA000256.

Pedersen, A., Decreau, P., Escoubet, C.-P., Gustafsson, G., Laakso, H., et al., 2001, Four-point high time resolution information on electron densities by the electric field experiments (EFW) on Cluster, *Ann. Geophys.* **19**:1483–1489.

Sandel, B. R., Broadfoot, A. L., Curtis, C. C., King, R. A., Stone, T. C., et al., 2000, The extreme ultraviolet imager investigation for the IMAGE mission, *Space Sci. Rev.* **91**:197.

Sandel, B.R., King, R. A., Forrester, W. T., Gallagher, D. L., Broadfoot, A. L. and Curtis, C. C., 2001, Initial results from the IMAGE extreme ultraviolet imager, *Geophys. Res. Lett.* **28**:1439.

Santolík, O., Lefeuvre, F., Parrot, M., and Rauch, J. L. 2001, Complete wave-vector directions of electromagnetic emissions: Application to INTERBALL-2 measurements in the nightside auroral zone, *J. Geophys. Res.* **106**:13,191–13,201.

Santolík, O., Parrot, M., and Lefeuvre, F., 2003, Singular value decomposition methods for wave propagation analysis, *Radio Sci.* **38**(1):1010, doi: 10.1029/2000RS002523.

Santolík, O., and Gurnett, D. A., 2003, Transverse dimensions of chorus in the source region, *Geophys. Res. Lett.*, **30**(2):1031, doi: 10.1029/2002GL016178.

Sazhin, S. S. and Hayakawa, M., 1992, Magnetospheric chorus emissions: A review, *Planet. Space Sci.*, **40**(5):681–697.

Smith, A. J., and Nunn, D., 1998, Numerical simulation of VLF risers, fallers, and hooks observed in Antarctica, *J. Geophys. Res.*, **203**(A4):6771–6784.

Stix, T. H., 1992, *Waves in Plasmas*, Am. Inst. of Phys., New York.

Trakhtengerts, V. Y., 1999, A generation mechanism for chorus emission, *Ann. Geophys.* **17**:95–100.

Trakhtengerts, V. Y., and Rycroft, M.J., 2000, Whistler-electron interactions in the magnetosphere: new results and novel approaches, *J. Atmos. and Terres. Phys.* **62**:1719–1733.

Willes, A. J., 2002, Jovian S burst drift rates and S burst/L burst interactions in a phase-bunching model, *J. Geophys. Res.* **107**(A5):1061, doi: 10.1029/2001JA000282.